Steady and Time Dependent Study of Laminar Separation Bubble (LSB) behavior along UAV Airfoil RG-15

M Muhammed*, M Virk
Arctic Technology & Icing Research Group,
UiT – The Arctic University of Norway, Narvik, 8514, Norway

ABSTRACT

The flow around the Unmanned Arial Vehicle (UAV) operating at a low Reynolds number regime of the $O(10^5)$ is predominantly laminar and it leads to the formation of Laminar Separation Bubble (LSB). The pressure, shear stress, and heat flux distribution are considerably affected by LSB, which affects lift, drag, and pitching moment values. Most existing RANS (Reynolds-Averaged Navier-Stokes) turbulence models are built on the assumption of fully turbulent flow. Therefore, these models require additional transport equations or reformulations or specific transition information to predict the LSB observed in low Reynolds number transition flows. Steady and transient computational fluid dynamics simulations were done using the RANS based transition turbulence model to study the behavior of LSB on UAV airfoil RG-15. The transition turbulence model can predict the LSB with considerable accuracy. The steady state and time averaged simulation results are matching in the pre stall region but deviates after stalling. High amplitude velocity fluctuations were observed near regions of transition and separation.

1. INTRODUCTION

The operating environment of the manned aircraft flying at a high Reynolds number (Re) of $O(10^6)$ and above is typically dominated by turbulent flow. The flow separation is delayed under such conditions due to the action of viscous force, whereas the flow around the UAV operating at a low Re regime of the $O(10^5)$ is predominantly laminar and is sensitive to even mild pressure gradients. The previously attached laminar boundary layer starts separating from the surface due to adverse pressure gradients and reattaches at some distance downstream while transitioning into turbulent flow. The resulting separation bubble is termed a Laminar Separation Bubble (LSB) (1). Such separations are more prone to appear on the suction surface of the airfoil and can alter the effective airfoil shape and the behavior of the flow field. Low Reynolds number airfoils are so sensitive that even mild changes in the geometry and operating conditions can deteriorate their aerodynamic performance. The pressure, shear stress, and heat flux distribution are considerably affected by LSB, which can alter the lift, drag, pitching moment values and stalling behavior of airfoils (2, 3).

The occurrence of LSBs were first reported by Jones (3) in 1934 during his experimental investigations to understand the stalling behavior of aircraft wings. Several experimental investigations were then done by the successive researchers to understand the structure and behavior of LSB, a detailed review of such studies can be found in (4).

*Corresponding Author: manafaero@gmail.com

The studies done by Horton (5) in 1968 provided an insight into the physical mechanism of growth and bursting of the bubble. He also proposed a fundamental structure of the LSB as shown in Figure 1. The laminar boundary layer separates from the airfoil surface at point S and the transition to turbulent flow occurs at the maximum height of the separation bubble at point T′. The reverse flow near the wall is eventually eliminated by turbulent mixing, and the flow reattaches at point R. Such separation bubbles are termed as short laminar separation bubbles and has only local effect on pressure distribution. However, with increased incidence or reduced speed, the 'short' bubble may suddenly expand and 'burst' to form a 'long laminar separation bubble'. The long bubbles can remain as unattached free shear layer or reattaches at a long distance downstream, which has a global influence on pressure distribution (1). The nature of bursting decides the stalling behavior of the airfoil.

In 1953 Owen (6) first classified the LSB as “short” or “long” based on the ratio of length of the bubble, “l” (the distance between the separation onset and re attachment of the flow) and displacement thickness “δ_s”. Bubbles with value of $\frac{l}{\delta_s} = O(10^2)$ are referred to as “short” bubbles and those with $\frac{l}{\delta_s}$ of the order of $O(10^4)$ are considered as “long” bubbles. Later Gaster (7) in 1969 estimated the length of short LSB to be approximately 100 momentum thicknesses and the length of long LSB to be 1,000 momentum thicknesses or more. Tani (1) divided the LSB into "short" and "long" categories according to the influence of the surface pressure distribution. A small reduction in the size of the suction peak before to separation is the only change that short bubbles make to the pressure distribution. On the other hand, a long bubble has a significant impact on the pressure distribution, reducing the suction peak to a small value and increasing the size and magnitude of the constant pressure region downstream of separation. The dynamics of these bubbles can be greatly influenced by changes in the angle of attack and Re. With an increase in angle of attack, short bubbles contract and long bubbles expand. A decrease in Re causes both long and short bubbles to expand, but long bubbles expand at a much faster rate than short bubbles. Further, long bubbles are also associated with large-scale instability, whereas short bubbles are relatively stable (5). Thus, the size of the bubble has significant impact on the aerodynamic performance.

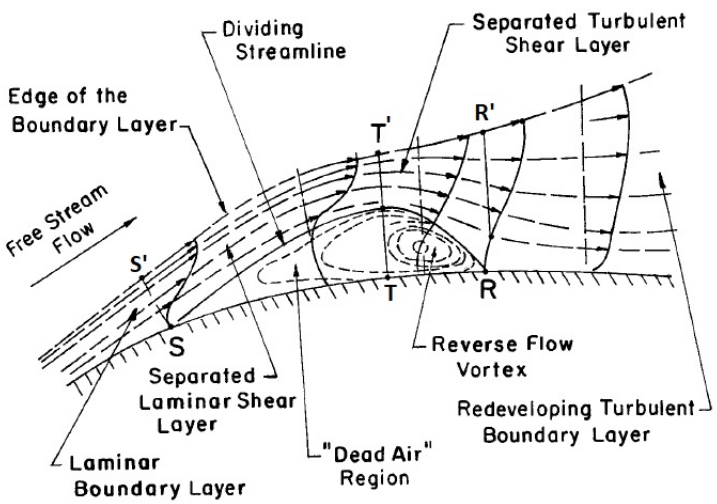

Figure 1: Fundamental structure of LSB (5)

Various experimental studies are done to understand the formation and characteristics of LSB was reviewed by Somashekar (8) and Park (9) and therefore are not repeated here. Instead, the current understanding of the characteristics of LSB and the studies validating the capability of RANS based turbulence model in predicting LSB is briefly reviewed. Laminar separation bubbles are so sensitive that even minor changes in operating conditions can affect their behavior. The location of separation, transition, and reattachment, as well as the length and thickness of the bubble, are all affected by environmental factors. These variations have considerable effect on the force coefficients (10) and shear stress distributions (11). In 1986 O'Meara (12) did investigations to understand the structure and behavior of LSB on NACA 663-018 airfoils at Reynolds numbers of the $O(10^4 - 10^5)$. The length and thickness of the LSB was found to be decreasing with Re and turbulence intensity, where as it is observed to increase with α. The separation point remains unchanged with Re but it moves upstream with α. In contrast with these observations Mitra (13) (E387 airfoil), Park (9) (DAE51 airfoil) and OO (14) (RG-15 airfoil) observed a decrease in bubble length with increasing α during their studies at Re of the $o(10^5)$. The point of separation, transition and reattachment were all observed to move upstream with α while the length of the LSB decreases (13). In 2008 Galbraith (11) reported that the transition location and reattachment locations move upstream with increasing Reynolds number based on his studies on SD7003 airfoil. Park (9) pointed out that the onset of separation moves downstream and the reattachment point moves upstream with increasing Re for those LSBs which failed to reattach on the surface, while the separation onset moves downstream for bubbles with reattachment point on the surface. Also, for low Reynolds number ($o(10^4)$) the bubble failed to reattach at small values of angle of attack ($5^0\ to\ 6^0$). The transition is initiated at a more upstream position as Re increases. The linear relationship between the length and thickness of LSB was also reported by Diwan (15).

The Laminar separation phenomenon can be simulated numerically using the Direct Numerical Simulations (DNS) and Large Eddy Simulations (LES) (11, 16-19). But such simulations are computationally expensive and is least favored by the industry. So, attempts have been made by researchers in utilizing the possibility of RANS based models to predict the laminar flow separation. Most existing Reynolds-Averaged Navier-Stokes (RANS) turbulence models are built on the assumption of assumption of fully turbulent flow. Therefore, these models require additional transport equations or reformulations or specific transition information to predict the LSB observed in low Reynolds number transition flows. Menter (20) in 2002 proposed the initial formulations of RANS based transition model capable of predicting LSB. Later in 2004 Menter (21) modified this transition model with an additional transport equation for $Re_{\theta t}$ coupled with SST $k - \omega$ turbulence model is known as $\gamma - Re_{\theta t}$ transition model. It is also called as transition $k - \omega$ SST turbulence model. The capability of this transition model in predicting the LSB over low Reynolds number airfoil RG-15 used for UAVs is studied in this paper using steady state and transient simulations. The predictions are validated with the experimental results obtained from literature.

2. COMPUTATIONAL METHODOLOGY

2.1. Computational Model

Numerical simulations were carried out using RG-15 airfoil, which is a low Reynolds number airfoil suitable for UAV applications. The chord of the reference airfoil was $C = 210\ mm$,which corresponds to a Reynolds number of 1.07×10^5 at an air velocity of $7.25\ m/s$. Numerical simulations were carried out using the commercial CFD software Ansys

FLUENT. 2-D multiblock structured C-grid was generated using ICEM CFD. The size of the domain is 10 times chord in all directions from the leading edge. The grid is refined sufficiently in the streamwise directions and a first cell of height of $1e^{-6}$ is used to ensure Y-plus value less than 1. The numerical grid having 2,31,032 is shown in Figure 2. The simulations were run for enough iterations to ensure convergence in force coefficients, location of LSB and residuals fall well below $1e^{-6}$. The studies were done for 6 different angle of attacks of $0, 3, 6, 9, 12\ and\ 15^o$ and the results are compared with the data available in literature (14). Transient simulations were performed using a time step value equal to $1e^{-5}$seconds for a total duration of 0.8 seconds. Grid independent studies are performed, and the fine grid is selected to capture the LSB dynamics accurately. Time step sensitivity is not performed as we adopt the grid and time step from literature (14) used for validation.

Transition $k\omega - SST$ turbulence model ($\gamma - Re_\theta\ transition\ model$) (22) couples the $SST\ k-\omega$ model with two more transport equations to account for the transition behavior. The transport equation for the intermittency to trigger the transition process and Momentum thickness Reynolds number transport equation for the transition onset criteria. A detailed description of the source terms and constants used in the turbulence model can be found in (23).

$$\frac{\partial}{\partial t}(\rho\gamma) + \frac{\partial}{\partial x_j}(\rho u_j \gamma) = \frac{\partial}{\partial x_j}[\left(\mu + \frac{\mu_t}{\sigma_\gamma}\right)\frac{\partial \gamma}{\partial x_j}] + P_{\gamma 1} - E_{\gamma 1} + P_{\gamma 2} - E_{\gamma 2} \quad (1)$$

$$\frac{\partial}{\partial t}(\rho Re_{\theta t}) + \frac{\partial}{\partial x_j}(\rho u_j Re_{\theta t}) = \frac{\partial}{\partial x_j}[\sigma_{\theta t}(\mu + \mu_t)\frac{\partial Re_{\theta t}}{\partial x_j}] + P_{\theta t} \quad (2)$$

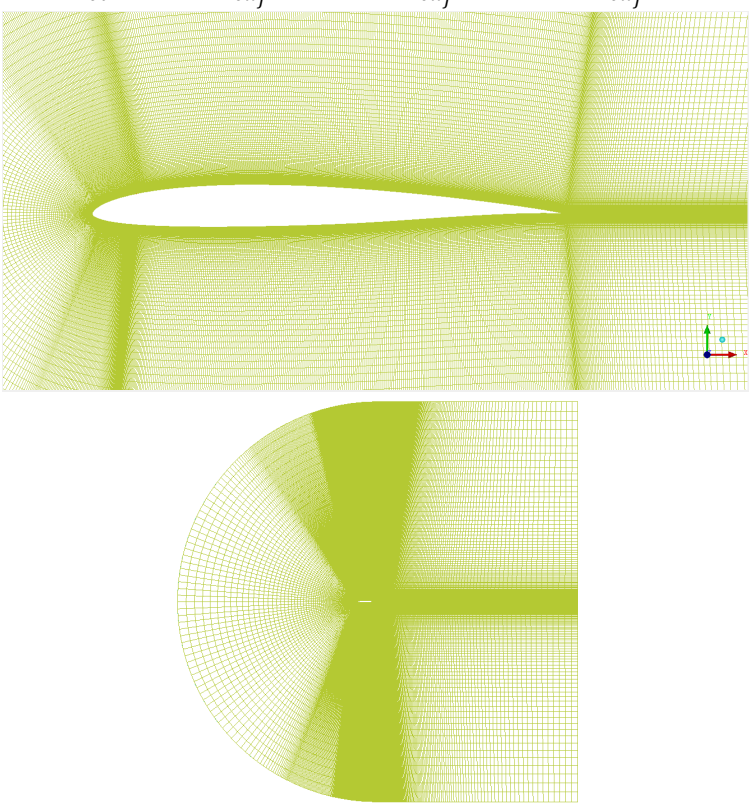

Figure 2: Computational domain and mesh over RG-15 Airfoil

3. RESULTS AND DISCUSSION

3.1. Comparison of $k-\omega$ SSt and Transition $k-\omega$ SST model

The behavior of LSB on RG-15 airfoil is studied at various angle of attack using steady state numerical simulations. CFD simulations were performed by employing $k-\omega$ SST turbulence model and transition $k-\omega$ SST turbulence model ($\gamma - Re_\theta\ transition\ model$). $k-\omega$ SST turbulence model failed to predict the LSB on the surface of the airfoil, whereas it is predicted on the suction side of the airfoil by transition $k-\omega$ SST turbulence model. The C_p and C_f distribution over RG-15 airfoil at 0, 3, and 6 degree angles of attack are shown in Figure 3 and Figure 4 respectively. Since pressure is constant inside the separation bubble, a flattening of C_p distribution curve indicates the region of LSB. The skin friction coefficient (C_f) shows negative values in the region of separation and has a peak value at the point of transition. The start of C_p flattening or the first zero crossing point of the C_f curve is considered as the point of separation onset and the point where the flattening of the C_p curve ends or the point where the peak negative value of C_f appears is considered as the point of transition. The point where the C_p value regains the inviscid $C_p$value or the point where C_f gains positive value is taken as the point of reattachment. Neither the C_p plateau nor the negative C_f is observed at angle of attack from 0-6 deg for simulations performed using $k-\omega$ SST turbulence model. On the other hand, transition $k-\omega$ SST turbulence model is successful in predicting the C_p plateau and the negative C_f for all the angle of attacks considered. The numerical simulation results are validated with the results obtained from the experimental studies of Oo et al. (14). It can be observed from Figure 3 that the experimental C_p distribution matched reasonably well with the predictions of transition $k-\omega$ SST turbulence model, whereas the $k-\omega$ SST turbulence model failed to predict the C_p accurately. It should be noted that the C_p predictions of $k-\omega$ SST turbulence model deviates from the experimental predictions mainly in the vicinity of LSB. The black dash dotted, and dotted lines shown in Figure 4 indicates the experimental prediction of regions of separation and reattachment. But $k-\omega$ SST turbulence model failed to predict any separated flow in these regions. The minor deviations observed in the C_P prediction of transition $k-\omega$ SST turbulence model can be due to the difference in the separation and reattachment locations. The capability of transition $k-\omega$ SST turbulence model in predicting the LSB is discussed in the coming section. This clearly indicates that the $k-\omega$ SST turbulence model is not suitable to study low Reynolds number flows involving LSB.

The effect of laminar separation bubble on aerodynamic coefficients: Coefficient of lift (C_L) and Coefficient of drag (C_D) are shown in Figure 5. The lift coefficient is more affected by the LSB than the drag coefficient. Considerable difference in the predictions between the turbulence models were observed at fully separated angle of attacks. At angle of attacks in which LSB is observed, the lift coefficient prediction differs by less than 10% except at 0-degree angle of attack. This can be due the presence of trailing edge separation bubble observed at this angle of attack, which is not predicted by $k-\omega$ SST turbulence model. The

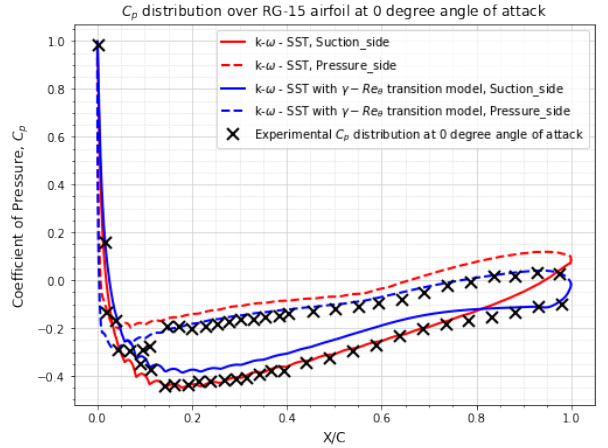

(a)

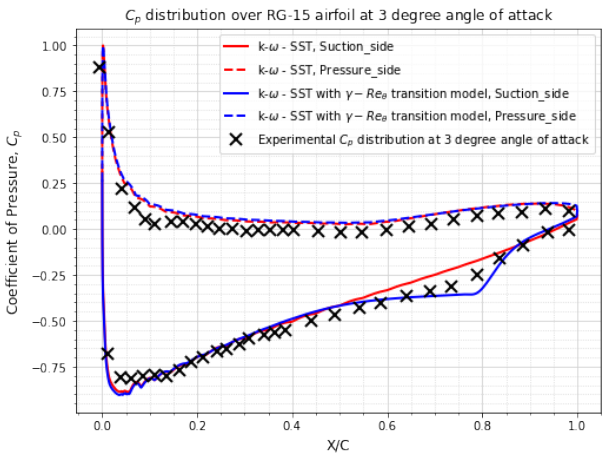

(b)

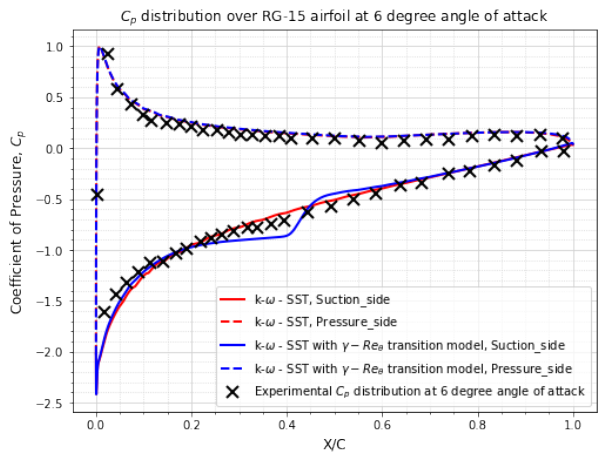

(c)

Figure 3: Coefficient of pressure distribution over Rg-15 airfoil at a) 0 degree, b) 3 degree and c) 6 degree angles of attack.

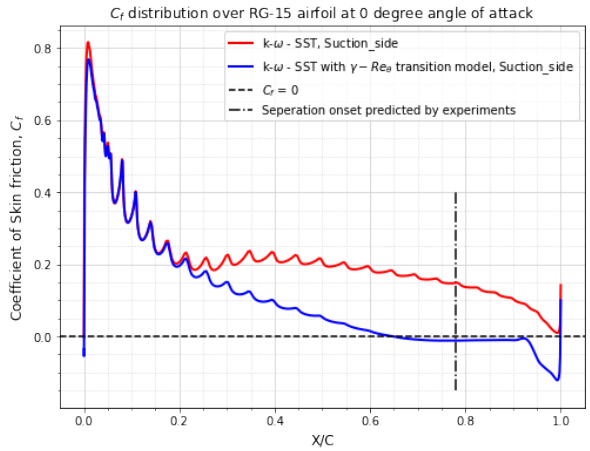

(a)

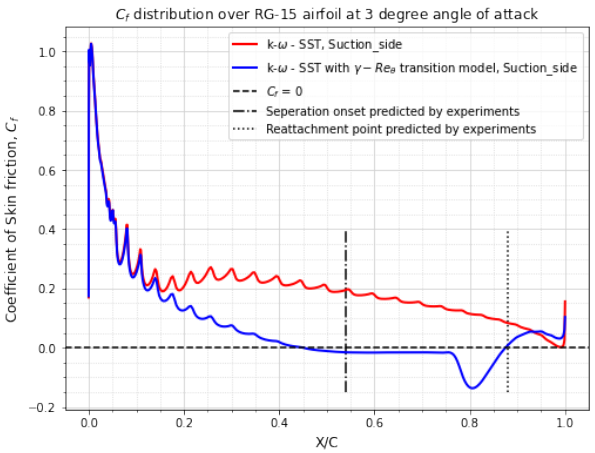

(b)

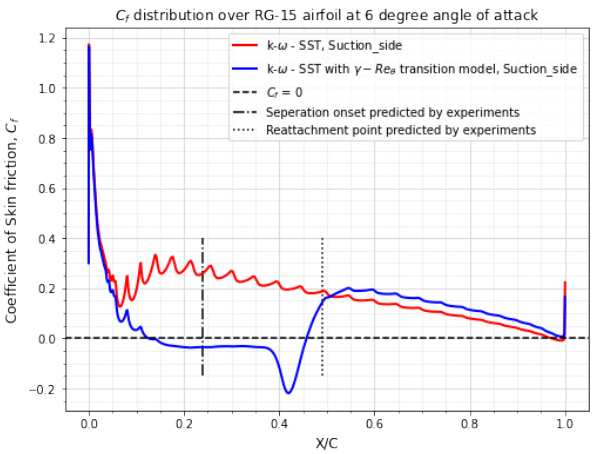

(c)

Figure 4: Coefficient of skin friction over Rg-15 airfoil at a) 0 degree, b) 3 degree and c) 6 degree angles of attack

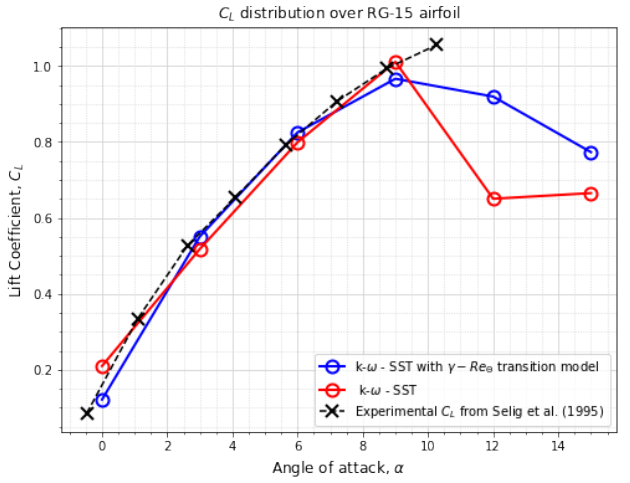

(a)

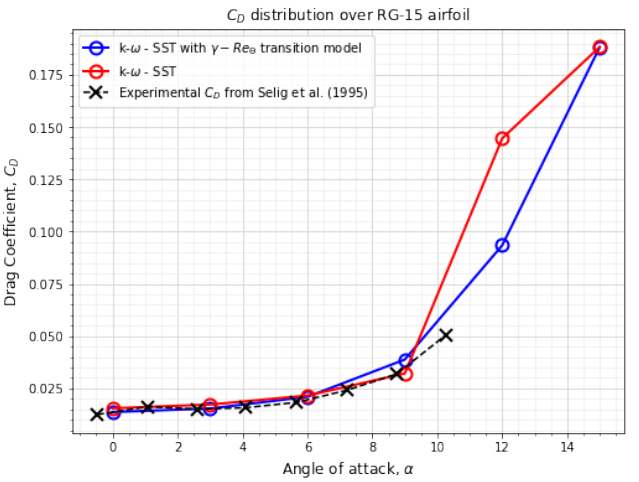

(b)

Figure 5: Coefficient of lift (left) and drag (right) using k-ω SST and Transition k-ω SST models.

presence of trailing edge LSB reduces the lift considerably. Experimental values of aerodynamic coefficients obtained from the experimental studies of Selig et al. (24) are compared with the numerical predictions in Figure 5. The aerodynamic coefficients predicted by transition k-ω SST turbulence model matches well with the experimental values in the pre-stall region, where are the experimental values are closer to the predictions k-ω SST turbulence model in the near stall region. This is due to the fact that that at higher angles of attack the flow behavior is dominated by turbulent flow characteristics than laminar flow. Both numerical models failed to predict the coefficients in the post stall region due to the modelling limitation of RANS models in the fully separated flow regime.

3.2. Validation of transition $k-\omega$ SST turbulence model

The validation of C_p distribution predicted by this turbulence model is already discussed in the previous section. This section focuses on the capability of transition $k-\omega$ SST turbulence model in predicting the LSB by comparing the separation and reattachment location with experimental and LES simulation results produced by Oo et al (14). Table 1 shows the separation and reattachment locations for various angles of attack predicted from experiments, LES and transition $k-\omega$ SST turbulence model. The simulations based on transition $k-\omega$ SST turbulence model results in the prediction of early separation and reattachment. The reattachment location is predicted more accurately by the model than the separation point, that the maximum difference in prediction when compared to experiments is 8% only (2% in comparison with LES). On the other hand, the flow separation is predicted 37 % earlier than experiments and 23 % earlier than LES. The maximum percentage difference is observed at 6-degree angle of attack and the difference is less at lower angles of attack. Similar information can be inferred from the skin friction coefficient distribution shown in Figure 4.

Table 1: Location of Separation and Reattachment for steady state simulations

AOA	Experiment		LES		Transition model		% Difference Experiment		% Difference LES	
	S(X/C)	R(X/C)	S(X/C)	R(X/C)	S(X/C)	R(X/C)	S(X/C)	R(X/C)	S(X/C)	R(X/C)
0	0.78	-	0.702	-	0.65	-	-16.67	-	-7.41	-
3	0.54	0.88	0.546	0.88	0.46	0.875	-14.81	-0.57	-15.75	-0.57
6	0.24	0.49	0.196	0.44	0.15	0.45	-37.50	-8.16	-23.47	2.27

3.3. Behavior of LSB on the surface of RG-15 airfoil at various angle of attack

The behavior of LSB on the surface of RG-15 airfoil with increase in angle of attack is shown in Figure 6. At an attack angle of zero degrees, a laminar separation bubble of open type is predicted near the trailing edge at x/c=0.65. Increasing the angle of attack by three degrees causes the onset of separation to move upstream at x/c=0.46 and the flow reattaches on the airfoil surface at x/c=0.875. As the angle of attack increases from three to six and nine degrees, the separation bubble moves upstream, and its length decreases from 0.417 C to 0.3 C and 0.087 C respectively. At 9 degree a small separation bubble is formed near the leading edge with flow reattaches at x/c=0.09. Then the flow separates again near the trailing edge at x/c=0.884. Similar but smaller separations were predicted by $k-\omega$ SST turbulence model also. At 12 degrees the flow separates at the leading edge and shows some tendency to reattach at x/c=0.14, but a thin layer of separated flow region exists till x/c=0.38 and then an open turbulent separation bubble is formed. Turbulent separation bubble starting from leading edge is predicted by $k-\omega$ SST turbulence model at this angle of attack. From Figure 5 it can be observed that the flow stalls at 9-degree angle of attack and the performance of RANS based turbulence models in the pre and post stall regions are not reliable (25, 26). Thus, the special flow separation behavior observed at these angles of attack need to be validated with experiments or LES/DNS simulations. The flow become fully separated from the leading edge for 15-degree angle of attack and an open turbulent bubble is formed without reattachment.

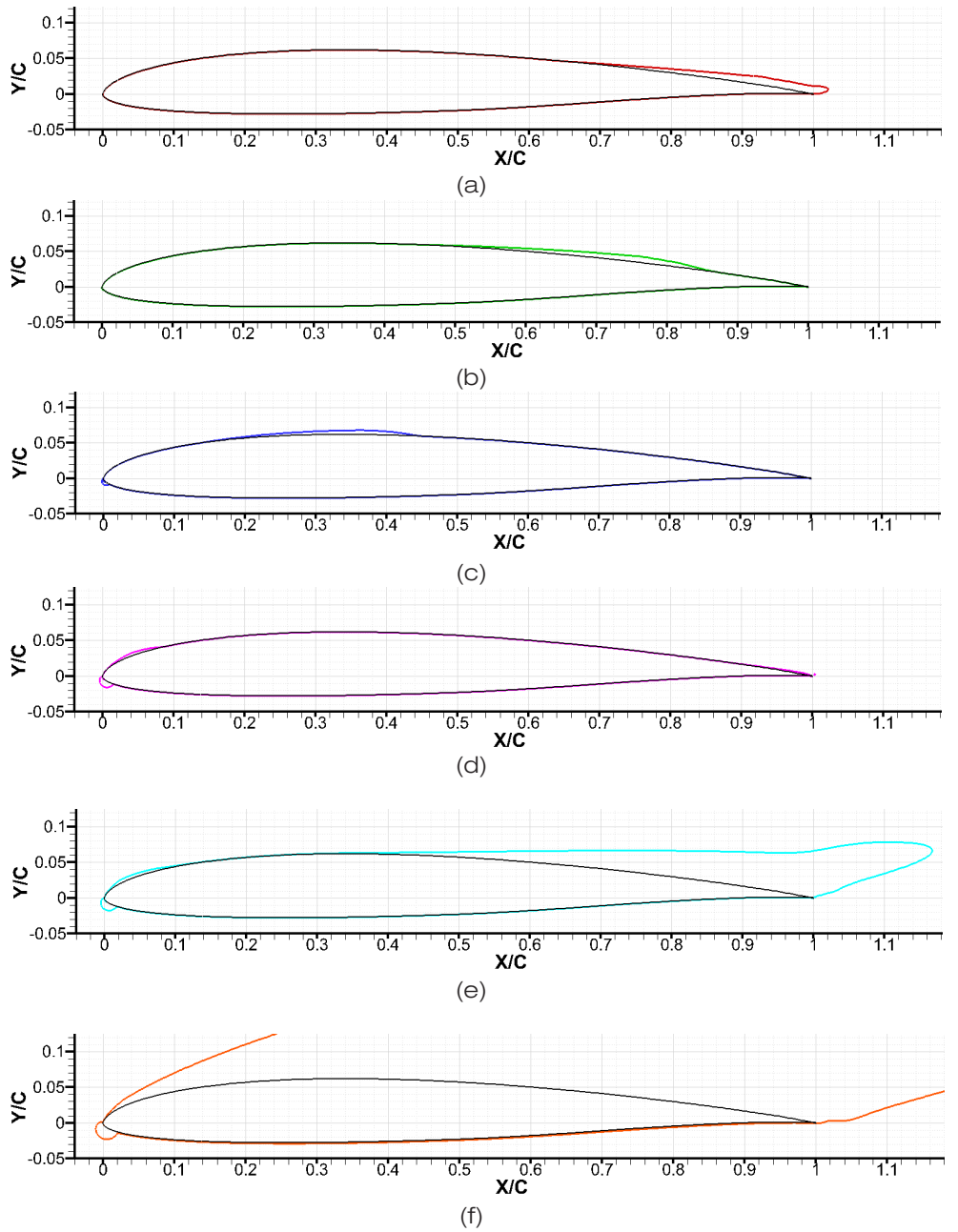

Figure 6: LSB on RG-15 airfoil at (a) 0 deg, (b) 3 deg, (c) 6 deg, (d) 9 deg, (e) 12 deg, & (f) 15 deg angles of attack

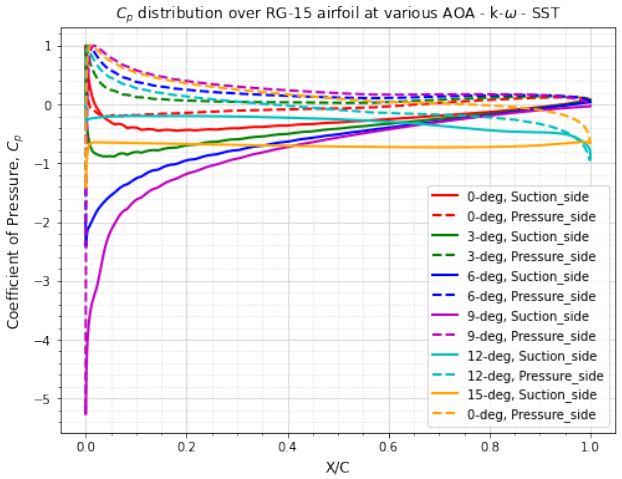

(a)

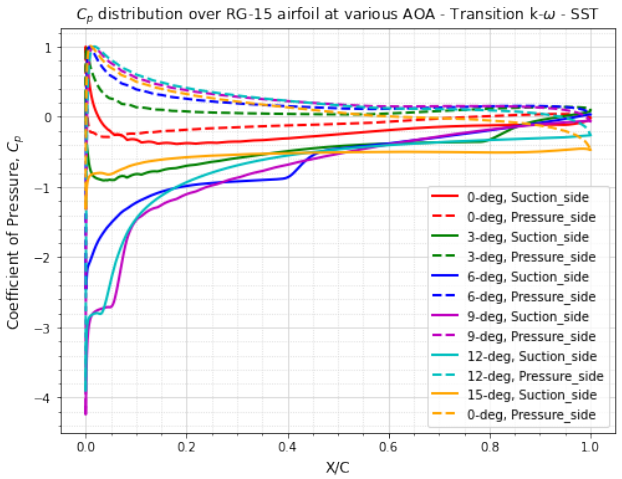

(b)

Figure 7: Coefficient of pressure using k-ω SST (left) and Transition k-ω SST (right) models.

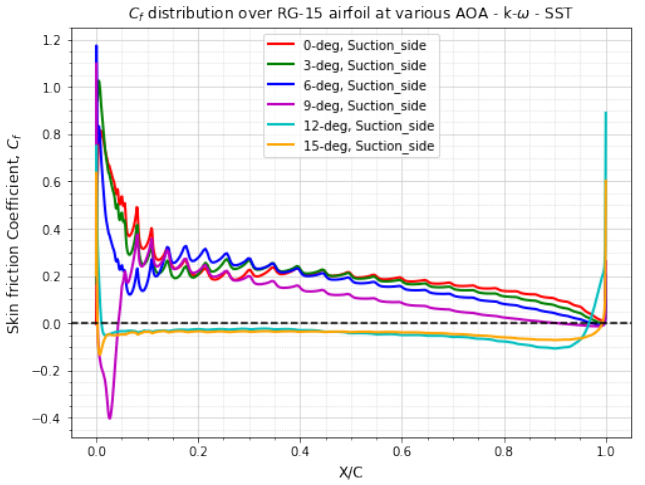

(a)

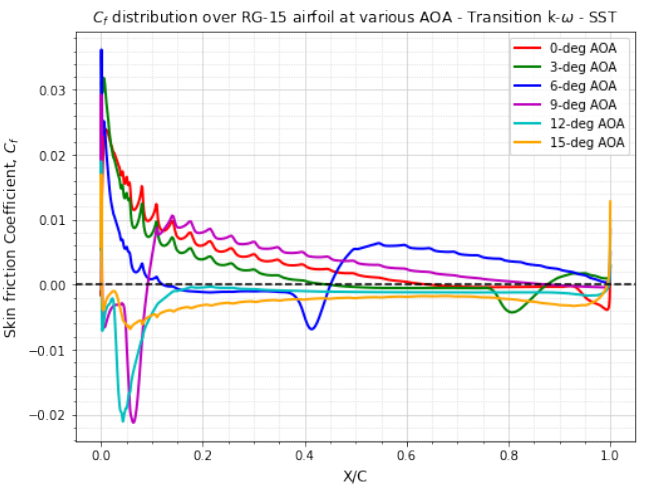

(b)

Figure 8: Coefficient of skin friction using k-ω SST (left) and Transition k-ω SST (right) models.

The peak negative value of C_f appears at the point of transition and it can be observed that the peak value increases with increase in angle of attack from 0-9 degree (see Figure 8). Also, as we move from 0 – 9 degrees, the C_f recovery occurs at a much faster rate that the flow reattaches faster. This can be due to the fact that the turbulent flow gains more energy with increase in angle of attack. Therefore, the size of the turbulent flow region (between T and R in Figure 1) inside the LSB decreases with angle of attack. This is also evident from the faster pressure recovery at higher angle of attacks as shown in Figure 7.

4. COMPARISON OF STEADY AND TIME AVERAGED RESULTS.

Limitations of $k-\omega$ SST turbulence model in predicting the separation and reattachment locations of LSB is evident from the previous section. The LSBs are highly unsteady in nature and therefore transient CFD simulations were performed using transition $k-\omega$ SST turbulence model to obtain the time averaged results. Compared to the steady state simulations the time averaged results predict the onset of separation more accurately, but the reattachment location is more accurately predicted in the steady state simulations (see Table 2). At 9 degree angle of attack the second flow separation is observed near the trailing edge at $x/c = 0.91$. A comparison of the steady state and transient C_p and C_f distribution at various angles of attack is shown in Figure 9 and Figure 10 respectively. The variation in the C_p distribution predicted by the steady and time averaged results are matching except for the 6 degree and 12 degrees angles of attack. This can be due to the significant vortex roll up movements observed at these angles of attack. Similar variations are observed for the C_f distribution also except for the difference in the location of separation and reattachment. Further, the magnitude of C_f predicted by time average results are less than that of steady state. Figure 11 shows the comparison of steady state and time averaged aerodynamic coefficients. The difference in C_L and C_D predictions are observed only in the post stall region and are matching quite well in the pre stall region.

Table 2: Location of Separation and Reattachment for Transient simulations

AOA	Transition model Unsteady		% Difference Experiment		% Difference LES	
	S(X/C)	R(X/C)	S(X/C)	R(X/C)	S(X/C)	R(X/C)
0	0.715	-	-8.33	-	1.85	-
3	0.525	0.89	-2.78	1.14	-3.85	1.14
6	0.218	0.42	-9.17	-14.29	11.22	-4.55

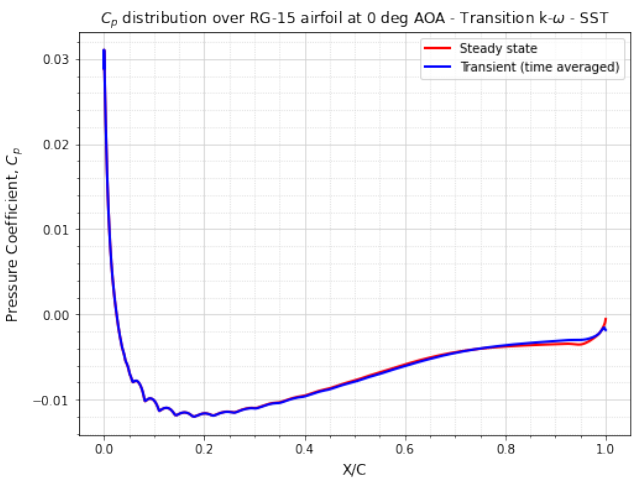

(a)

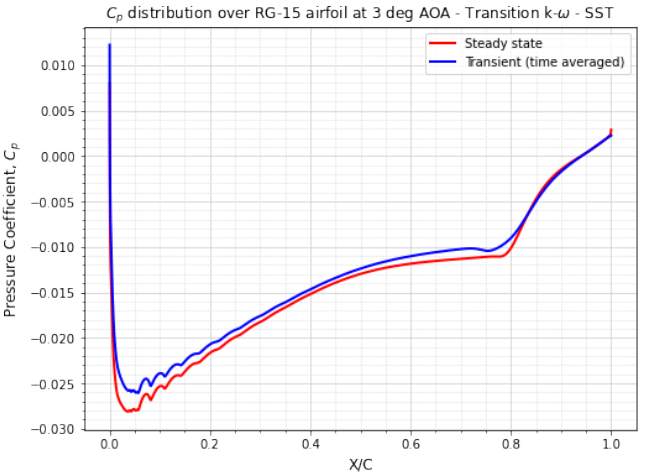
C_p distribution over RG-15 airfoil at 3 deg AOA - Transition k-ω - SST
Steady state
Transient (time averaged)
Pressure Coefficient, C_p
X/C

(b)

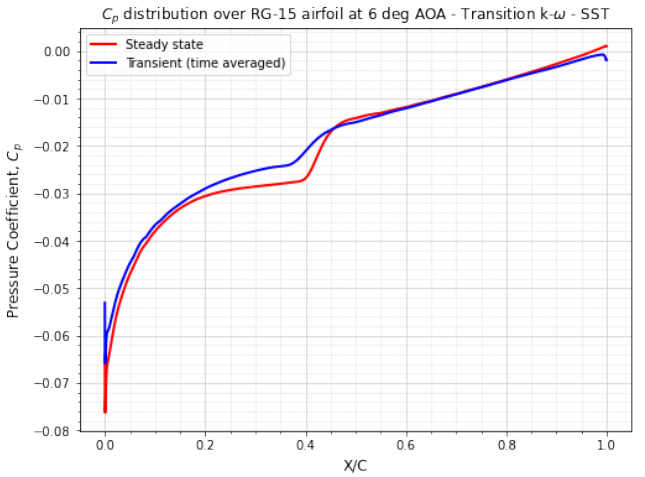
C_p distribution over RG-15 airfoil at 6 deg AOA - Transition k-ω - SST
Steady state
Transient (time averaged)
Pressure Coefficient, C_p
X/C

(c)

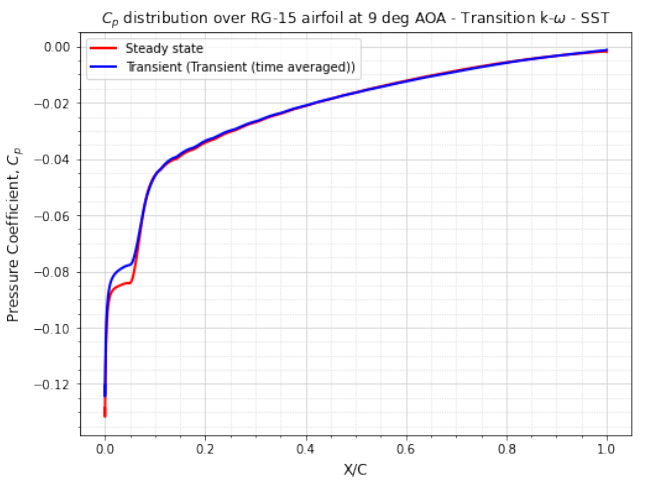
C_p distribution over RG-15 airfoil at 9 deg AOA - Transition k-ω - SST
Steady state
Transient (Transient (time averaged))
Pressure Coefficient, C_p
X/C

(d)

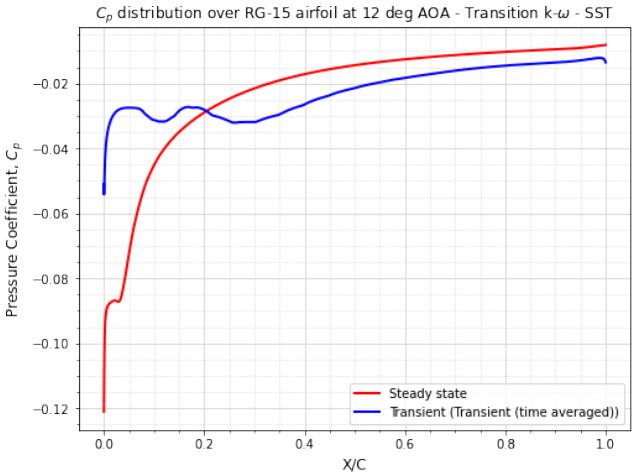

(e)

Figure 9: Comparison of C_p distribution predicted by steady and transient simulations at various AOA

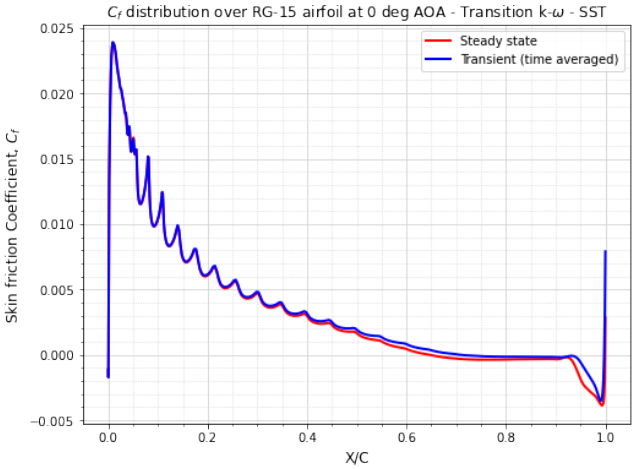

(a)

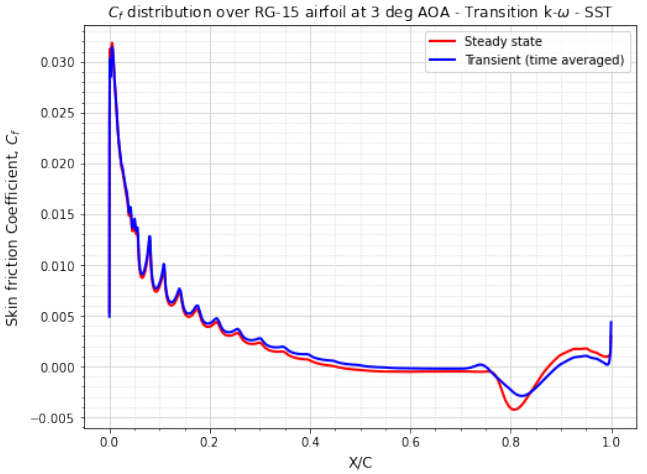
C_f distribution over RG-15 airfoil at 3 deg AOA - Transition k-ω - SST
Steady state
Transient (time averaged)
Skin friction Coefficient, C_f
0.030
0.025
0.020
0.015
0.010
0.005
0.000
−0.005
0.0
0.2
0.4
0.6
0.8
1.0
X/C

(b)

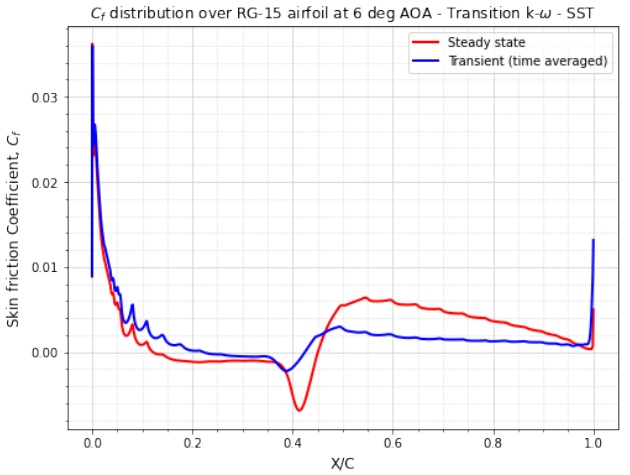
C_f distribution over RG-15 airfoil at 6 deg AOA - Transition k-ω - SST
Steady state
Transient (time averaged)
Skin friction Coefficient, C_f
0.03
0.02
0.01
0.00
0.0
0.2
0.4
0.6
0.8
1.0
X/C

(c)

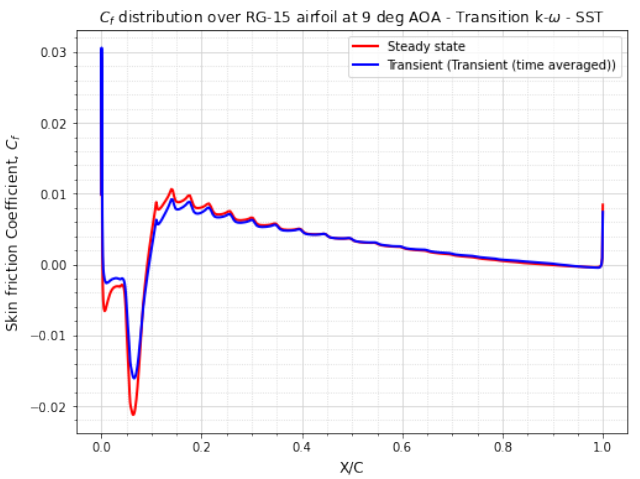
C_f distribution over RG-15 airfoil at 9 deg AOA - Transition k-ω - SST
Steady state
Transient (Transient (time averaged))
Skin friction Coefficient, C_f
0.03
0.02
0.01
0.00
−0.01
−0.02
0.0
0.2
0.4
0.6
0.8
1.0
X/C

(d)

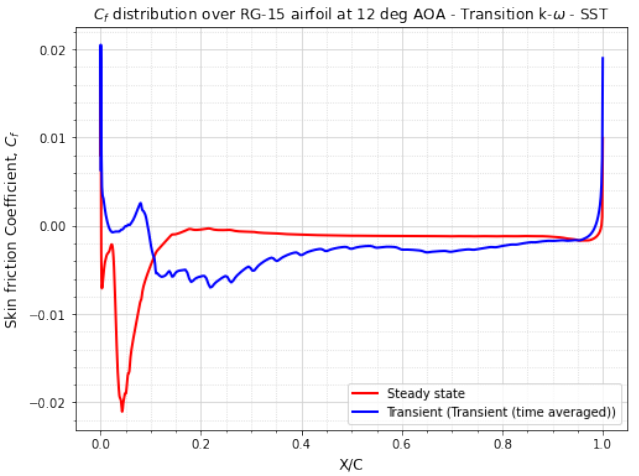

(e)

Figure 10: Comparison of C_f distribution predicted by steady and transient simulations at various AOA

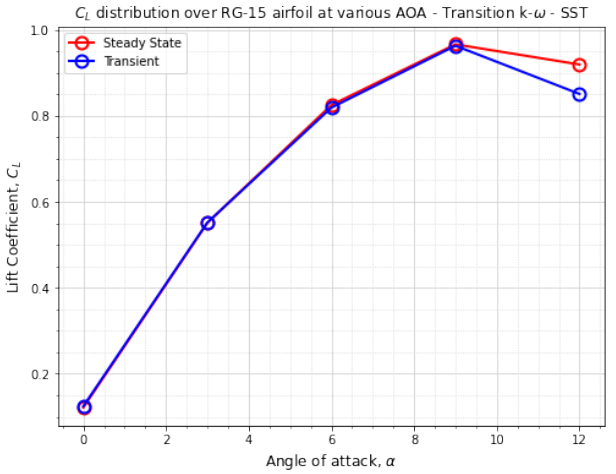

(a)

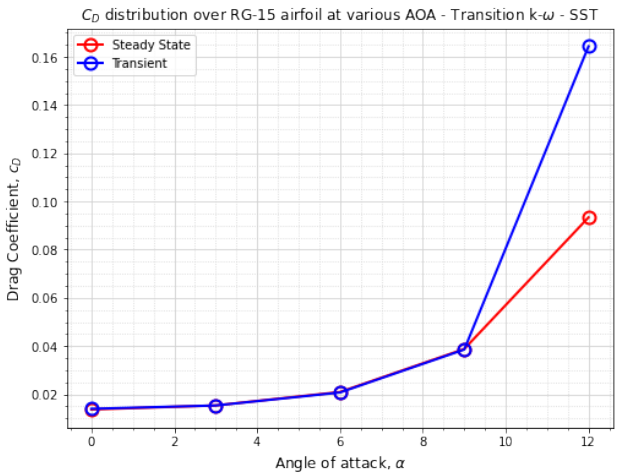

(b)

Figure 11: Coefficient of lift (left) and drag (right) using steady and transient simulations

3.5. Spectral analysis of turbulent fluctuations

RANS based simulations are not suitable to understand the turbulence statistics quantitatively, because of the averaging process. But it can be used to understand the turbulence qualitatively to identify the regions of turbulent flow. An attempt is made in this study to understand the turbulent fluctuations along the laminar separation bubble. LSB formed at 6 degrees angle of attack is selected because of the presence of a closed bubble on the surface of airfoil at this angle of attack. Figure 12 (a) to (f) corresponds to the turbulent spectra at six points marked on Figure 12 (g) in order from left to right. It can be observed that the turbulent fluctuations increased considerably at the pre and post transition regions. High amplitude velocity fluctuations are more near the regions of transition with its amplitude reaches maximum at transition and downstream. LES/DNS simulations are required to understand the phenomenon in detail.

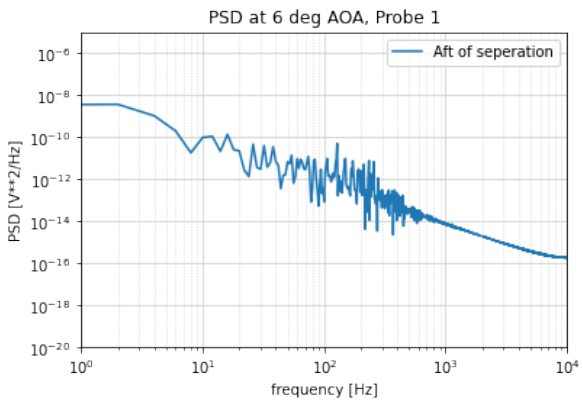

(a)

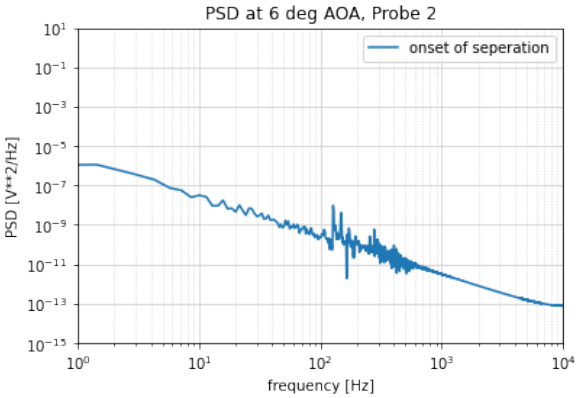
PSD at 6 deg AOA, Probe 2
onset of seperation
PSD [V**2/Hz]
frequency [Hz]

(b)

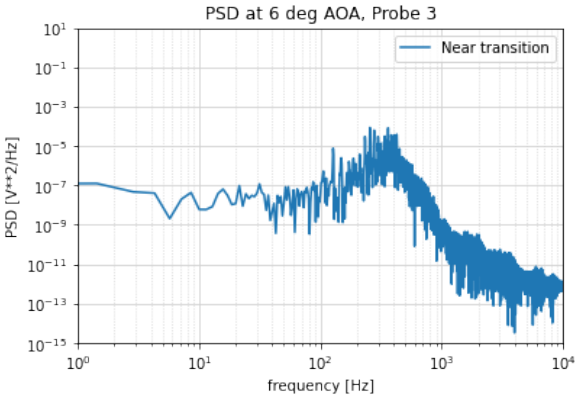
PSD at 6 deg AOA, Probe 3
Near transition
PSD [V**2/Hz]
frequency [Hz]

(c)

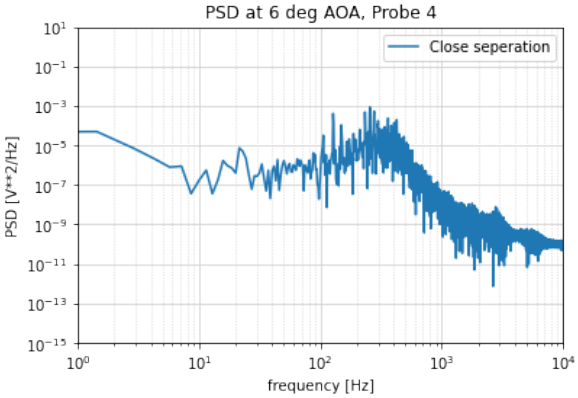
PSD at 6 deg AOA, Probe 4
Close seperation
PSD [V**2/Hz]
frequency [Hz]

(d)

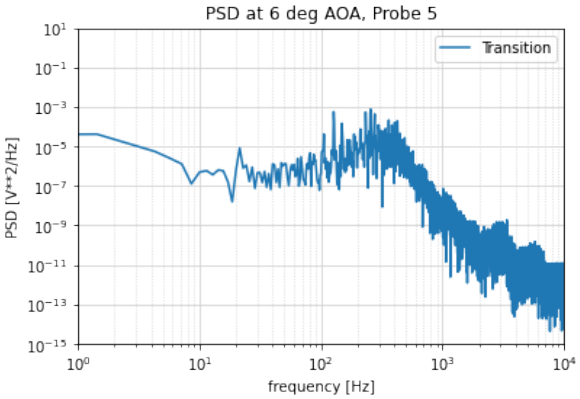

(e)

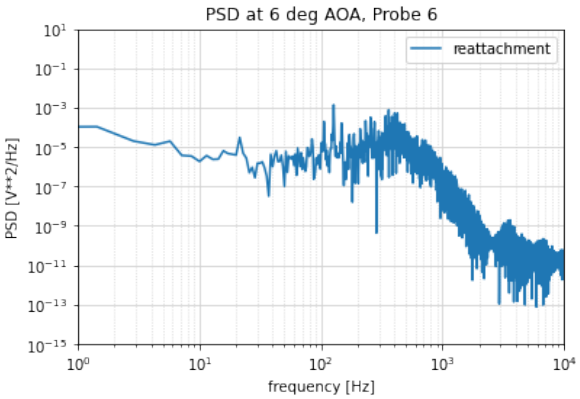

(f)

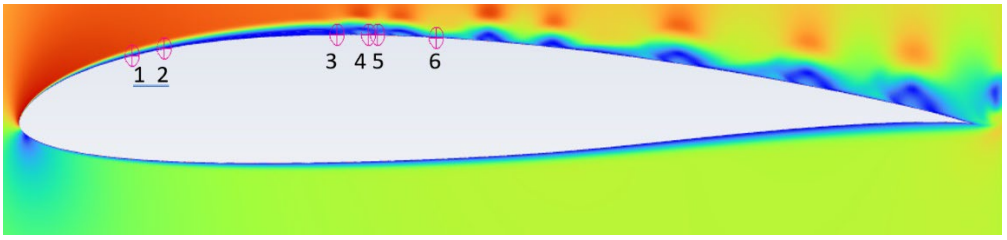

(g)

Figure 12: Velocity spectra at various points inside LSB for 6 deg AOA. Figure (a) to (f) corresponds to points 1-6 marked in figure (g) in order from left to right.

4. CONCLUSION

Numerical simulations using $k-\omega$ SST and transition $k-\omega$ SST turbulence models are performed to assess its ability to predict the laminar separation bubble over RG-15 airfoil at Reynolds number of 1.07×10^5. The predictions are compared with the experimental separation and reattachment locations available in the literature. The $k-\omega$ SST turbulence model is not capable of predicting the laminar separation bubble and a fully attached flow is predicted for lower angle of attacks. Transition $k-\omega$ SST turbulence model can predict the LSB, but the onset of separation is predicted early by this model. The LSB moves upstream with the increase in angle of attack along with a decrease in length and thickness of the separation bubble. Transient CFD simulations were performed using the transition model and the steady and time averaged results are compared. The onset of separation is predicted more accurately by the transient simulations, but better reattachment location predictions are observed for steady state simulations. Spectral analysis of velocity fluctuations indicate that the velocity fluctuations are more at regions of transition and reattachment because of the turbulent nature of the flow.

ACKNOWLEDGEMENT

The work reported in this paper is supported by the UiT- The Arctic University of Norway (Project no- 7400-72104) & nICE project of UiT & Research Council of Norway (Project no-324156).

REFERENCES

[1] Tani I. Low-speed flows involving bubble separations. Progress in Aerospace Sciences. 1964; 5:70-103.

[2] Hain R, Kähler C, Radespiel R. Dynamics of laminar separation bubbles at low-Reynolds-number aerofoils. Journal of Fluid Mechanics. 2009; 630:129-53.

[3] Jones BM. Stalling. The Aeronautical Journal. 1934;38(285):753-70.

[4] HORTON H, YOUNG A. Some results of investigations of separation bubbles (Flow separation bubble data, and comparisons with velocity and pressure measurements). 1966. 1966:779-811.

[5] Horton HP, editor Laminar separation bubbles in two and three dimensional incompressible flow1968.

[6] Owen PR, Klanfer L, editors. On the Laminar Boundary Layer Separation from the Leading edge of a Thin Aerofoil1953.

[7] Gaster M, editor The Structure and Behavior of Laminar Separation Bubbles1969.

[8] Somashekar V, Raj AS. Experimental Investigation on Laminar Separation Bubble Over an Airfoil–A Review. Indian Journal of Science and Technology. 2018;11(11):1-9.

[9] Park D, Shim H, Lee Y. PIV measurement of separation bubble on an airfoil at low Reynolds numbers. Journal of Aerospace Engineering. 2020;33(1):04019105.

[10] Bastedo WG, Mueller TJ. Spanwise variation of laminar separation bubbles on wings at low Reynolds number. Journal of Aircraft. 1986;23(9):687-94.

[11] Galbraith M, Visbal M. Implicit Large Eddy Simulation of Low-Reynolds-Number Transitional Flow Past the SD7003 Airfoil. 40th Fluid Dynamics Conference and Exhibit. Fluid Dynamics and Co-located Conferences: American Institute of Aeronautics and Astronautics; 2010.
[12] OMEARA M, MUELLER T, editors. Experimental determination of the laminar separation bubble characteristics on an airfoil at low Reynolds numbers. 4th Joint Fluid Mechanics, Plasma Dynamics and Lasers Conference; 1986.
[13] Mitra A, Gokul P, Ramesh O, editors. The Role of laminar separation bubble on low Reynolds number airfoils. 51st AIAA Aerospace Sciences Meeting including the New Horizons Forum and Aerospace Exposition; 2013.
[14] Oo NL, Richards PJ, Sharma RN. Ice-Induced Separation Bubble on RG-15 Airfoil at Low Reynolds Number. AIAA Journal. 2020;58(12):5156-67.
[15] Diwan SS, Ramesh ON. On the origin of the inflectional instability of a laminar separation bubble. Journal of Fluid Mechanics. 2009;629:263-98.
[16] Spalart PR, Strelets MK. Mechanisms of transition and heat transfer in a separation bubble. Journal of Fluid Mechanics. 2000;403:329-49.
[17] Yuan W, Khalid M, Windte J, Scholz U, Radespiel R. An Investigation of Low-Reynolds-Number Flows Past Airfoils. 23rd AIAA Applied Aerodynamics Conference.
[18] Catalano P, Tognaccini R. Influence of Free-Stream Turbulence on Simulations of Laminar Separation Bubbles2009.
[19] Catalano P, Tognaccini R. Turbulence modeling for low-Reynolds-number flows. AIAA journal. 2010;48(8):1673-85.
[20] Menter F, Esch T, Kubacki S. Transition modelling based on local variables. Engineering Turbulence Modelling and Experiments 5: Elsevier; 2002. p. 555-64.
[21] Menter FR, Langtry RB, Likki S, Suzen Y, Huang P, Völker S. A correlation-based transition model using local variables—part I: model formulation. 2006.
[22] Langtry RB, Menter F. Correlation-Based Transition Modeling for Unstructured Parallelized Computational Fluid Dynamics Codes. AIAA Journal. 2009.
[23] Ansys I. Ansys Fluent Theory Guide2022.
[24] Selig MS. Summary of low speed airfoil data: SOARTECH publications; 1995.
[25] Nived MR, Mukesh BS, Athkuri SSC, Eswaran V. On the performance of RANS turbulence models in predicting static stall over airfoils at high Reynolds numbers. International Journal of Numerical Methods for Heat & Fluid Flow. 2022;32(4):1299-323.
[26] Abed B, Benzerdjeb A, Achache H, Debab A, Hamidou M-K, editors. Evaluation of Rans Turbulence Models for Turbulent Flow over Nrel S809 Airfoil2019.